~~Stanford~~ : PD4 to Bragg Gratings, Photosensitivity and Poling in Glass Fibers and Waveguides : Applications and Fundamentals Topical Meeting. Williamsburg, 194

1559

Improved Efficiency Narrow-Band Acoustooptic Tunable Reflector using Fibre Bragg Grating

W.F. Liu, L. Dong, L. Reekie, D.O. Culverhouse*

Optoelectronics Research Centre, University of Southampton, Southampton SO17 1BJ, UK

and

P.St.J. Russell

Optoelectronics Group, Department of Physics, University of Bath, Claverton Down, Bath BA2 7EB, UK

Abstract

We report a 90% efficient acoustooptic superlattice modulator in a fibre Bragg grating whose diameter is reduced by HF etching. The narrow-band amplitude-adjustable reflections are tunable over several nm.

* Present address: Corning Inc., Corning, N.Y. 14831, USA

Improved Efficiency Narrow-Band Acoustooptic Tunable Reflector using Fibre Bragg Grating

W.F. Liu, L. Dong, L. Reekie, D.O. Culverhouse
Optoelectronics Research Centre, University of Southampton, Southampton SO17 1BJ, UK

P.St.J. Russell
Optoelectronics Group, Department of Physics, University of Bath, Claverton Down, Bath BA2 7EB, UK

All-fibre versions of bulk devices are very attractive in fibre systems where low insertion loss is always desirable. We have greatly improved the performance of a recently reported [1] Bragg-grating-based acousto-optic superlattice modulator (AOSLM) by reducing the fibre diameter by HF etching. This improves the overlap of acoustic and optical power, resulting in modulator efficiencies as high as 90%. The modulator produces narrow-band amplitude-adjustable reflections that can be tuned over several nm, which is attractive for WDM and laser applications. In the device, an extensional acoustic wave is launched along a fibre Bragg grating. The ensuing superlattice modulation causes additional bands of reflection to appear on both sides of the Bragg condition. The device works by coupling together the forward and backward propagating Bloch modes in the grating (a principle first proposed in 1986 [2,3]) and operates in *reflection mode*. This differentiates the AOSLM from all previously reported acousto-optic fibre devices, which all rely on intermodal coupling, examples being LP_{01} to LP_{11} coupling in dual-mode [4] and twin-core [5] fibres, four-port null-couplers [6], polarisation mode couplers in Hi-Bi fibre [7] and guided-to-cladding mode coupling in standard telecom fibre [8]. In all these devices the intermodal beat length $L_B = \lambda/(n_1 - n_2)$ at optical wavelength λ between two modes with phase indices n_1 and n_2 is matched by the acoustic wavelength v_s / f_s where v_s and f_s are the acoustic phase velocity and frequency.

When an acoustic wave is launched along a fibre Bragg grating, narrow-band frequency-shifted reflections appear on either side of the Bragg condition. These can be regarded as the consequence of side-bands in spatial frequency ("ghost" gratings) which form in a periodically phase-modulated Bragg grating:

$$\varepsilon = n_0^2\left(1 + M\cos\left[Kz + \frac{Ks_o}{k_s}\sin(k_s z)\right]\right)$$

where $K = 2\pi/\Lambda$ is the Bragg grating vector (Λ being its pitch), k_s is the acoustic wavevector and $s_o = \sqrt{2P_s/(EAv_{gs})}$ is the peak strain induced by an acoustic wave of power P_s in a fibre of cross sectional area *A*, Young's modulus *E* and acoustic group velocity v_{gs}. The mean phase index of the optical guided modes is n_o.

Provided they are not too strong, these "ghost" gratings will have an effective bandwidth which equals that of a weak grating of the same physical length *L* as the

---

Present address: Corning Inc., Corning, N.Y. 14831, USA

Bragg grating, i.e., $\Delta\lambda_{opt} = 1.39\lambda^2/(\pi L n_o)$. The distance of their reflection maxima from the main Bragg peak is given approximately by:

$$\frac{c\Delta\lambda}{\lambda^2} \approx \Delta\nu = \frac{mcf_s}{2n_o v_s}$$

where m is the side-band order. This expression neglects the dispersion of the Bloch waves, which is very strong near the stop-band edges.

A guided mode, incident on a Bragg grating carrying a counter-propagating acoustic wave, is reflected into a counter-propagating mode with a frequency shift $\pm f_s$, which is *positive* on the short wavelength side ($\lambda < \lambda_B$) and *negative* when $\lambda > \lambda_B$. Thus the Doppler shift is sometimes reversed. As reported in [8], the superlattice reflection efficiency in the first side-band takes the approximate form:

$$\eta = \tanh^2\left[\kappa L \, \mathrm{J}_1\left(\frac{Ks_o}{k_s}\right)\right] = \tanh^2\left[\kappa L \, \mathrm{J}_1\left(\frac{\lambda_s}{\Lambda}\sqrt{\frac{2P_s}{EAv_{gs}}}\right)\right]$$

where κ is the coupling constant of the Bragg grating. For given drive power, the efficiency can be improved by minimising the fibre cross-sectional area *A*. This has the effect of increasing the acousto-optic overlap. We have achieved this by HF etching away the cladding glass and thus reducing its overall diameter. A substantially improved the device performance results.

The experimental set-up of the device is shown in figure 1. A planar piezoelectric transducer is bonded to the base of a fused silica horn, the point of the horn being fusion-spliced to the fibre. Electrical drive powers of up to a few hundred mW were applied. The single side-band purity of the frequency-shifted signal was tested by splitting the light from a tunable single frequency diode laser into two paths. One was frequency shifted by an 80 MHz Bragg cell, and the other was directed at the superlattice modulator. The signal reflected from the superlattice modulator was then mixed at a square-law detector with the 80 MHz shifted signal. As reported in [8], excellent single-side-band purity was obtained in all cases.

The reflection spectrum of the AOSLM with and without acoustic power was measured (Figure 2) using a broad band LED as source. Notice that, in addition to the two strong side-bands, two additional weak reflection bands are apparent. These are caused by higher order "ghost" gratings and are further confirmation of the strength of the superlattice effect. First side-band AOSLM reflectivities as high as ~90% have been obtained in a fibre etched to a final diameter of ~30 μm, the acoustic frequency being ~10 MHz. The grating had an index modulation of 10^{-3} (yielding $\kappa = 4\ \mathrm{mm}^{-1}$) and its length L = 3 mm. The tuning of side-band position with acoustic frequency (in a 10% device) is shown in figure 3, together with the theoretical prediction. Tuning over 2 nm is achieved for acoustic frequencies between 4 MHz and 15 MHz.

In conclusion, we report a highly efficient AOSLM using a fibre Bragg grating with an etched-away cladding. This device can function as an efficient frequency shifter in reflection mode with adjustable reflectivity. The optical bandwidth for the current device is in the region of ~0.2 nm. The turn-on and turn-off time of such device is limited by the propagation time of the acoustic wave in the device, which is of order 500 nsec for the current 3 mm long device. This suggests applications to Q-switching of fibre lasers at rates of up to a few MHz. The device can also act as a

tunable filter, a switch and an amplitude modulator.

References

1. W. F. Liu, P.St.J. Russell and L. Dong, Opt. Lett. **22** 1515 (1997)
2. P.St.J. Russell, J. Appl. Phys. **59** 596 (1986).
3. P.St.J. Russell, J. Mod. Opt **38** 1599 (1991).
4. B.Y. Kim, J.N. Blake, H.E. Engan and H.J. Shaw, Opt. Lett. **11** 389 (1986)
5. H. Sabert, L. Dong and P.St.J. Russell, Int.J. Optoeiectronics **7** 189 (1992).
6. Reviewed in: T.A. Birks, D.O. Culverhouse and P.St.J. Russell, J. Lightwave Techn. **14** 2519 1996
7. M. Berwick, C.N. Pannell, P.St.J. Russell and D.A. Jackson, Elect. Lett. **27** 713 (1991).
8. H.S. Kim, S.H. Yun, I.K. Hwang, B.Y. Kim, Optical Communications Conference, PD7 (1997).

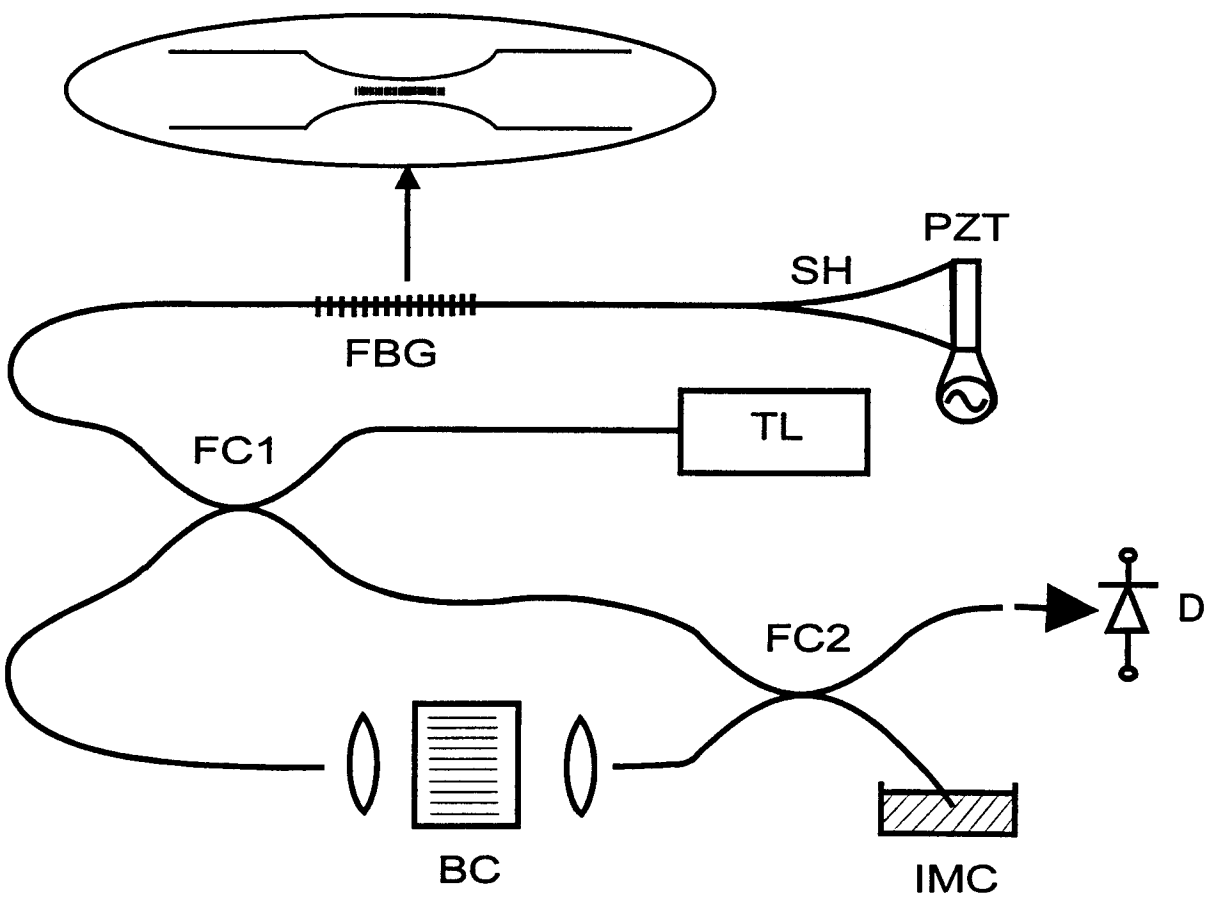

Figure 1 Experimental set-up. TL: tunable single frequency diode laser. D: square-law detector. SH: silica horn. FBG: fibre Bragg grating. FC: 3 dB fused coupler. BC: Bragg cell. IMC: Index matching fluid.

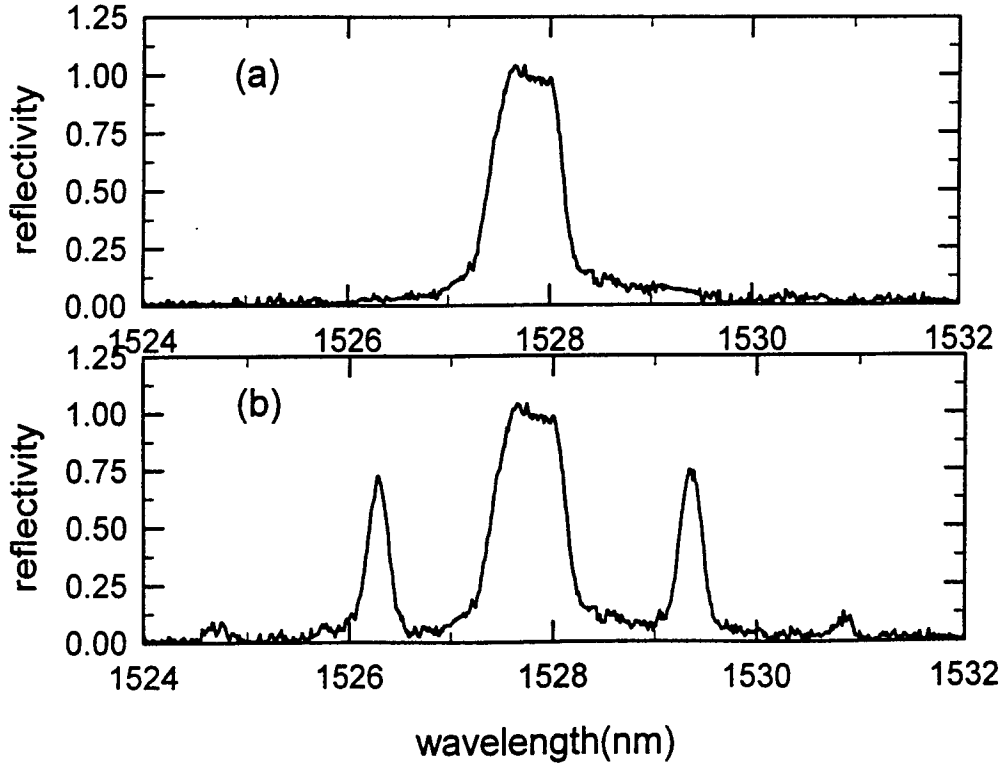

Figure 2 The reflection spectrum of the original grating (top) and that of the grating with acoustic wave applied (bottom).

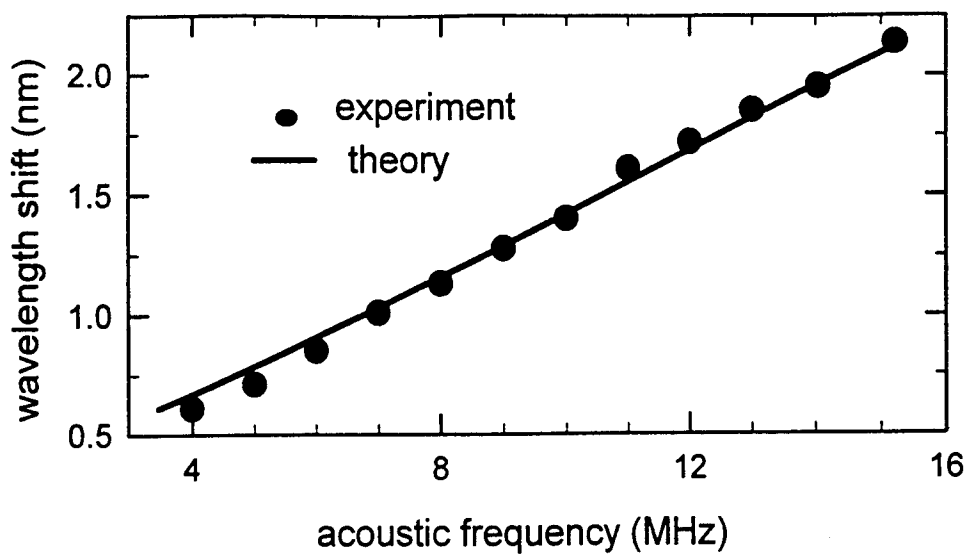

Figure 3 Position of the first order side-lobe as a function of acoustic frequency. The line is the theoretical prediction.